

## Case Series

# Polyomavirus-associated Disseminated T-cell Lymphoma in a Colony of Zebra Finches (*Taeniopygia guttata*)

Katherine A Shuster,<sup>1\*</sup> Tzushan S Yang,<sup>1</sup> Kate T Snyder,<sup>2</sup> Nicole Creanza,<sup>2</sup> Patrick K Mitchell,<sup>3</sup> Laura B Goodman,<sup>3</sup> Jennifer K Grenier,<sup>4</sup> Nicholas M Tataryn,<sup>1</sup> Lauren E Himmel,<sup>1</sup> and Katherine N Gibson-Corley<sup>1</sup>

Four zebra finches in a closed research colony presented with variable clinical signs, including masses, skin lesions, shivering, and/or ruffled feathers. These birds were not responsive to treatment efforts; 3 died and one was euthanized. All 4 were submitted for necropsy to determine the cause of the clinical signs. Gross necropsy and histopathologic findings from all birds resulted in a diagnosis of round cell neoplasia in multiple organs, including the skin, liver, kidney, and reproductive tract, with intranuclear inclusion bodies in the neoplastic cells. In all 4 cases, immunohistochemical staining showed strong immunoreactivity for CD3 in 70% to 80% of the neoplastic round cells, with a relatively small subset that were immunopositive for Pax5. These findings supported a diagnosis of T-cell lymphoma. Frozen liver tissue from one case was submitted for next-generation sequencing (NGS), which revealed viral RNA with 100% sequence homology to canary polyomavirus strain 34639 that had originally been identified in a European goldfinch. Formalin-fixed paraffin-embedded scrolls from another case were also submitted for NGS, which revealed viral RNA with 97.2% sequence homology to canary polyomavirus strain 37273 that had originally been identified in a canary. To localize the virus in situ, RNAscope hybridization was performed using a probe designed to target the VP1 gene of the sequenced virus in frozen liver tissue. In all 4 cases, disseminated and robust hybridization signals were detected in neoplastic cells. These findings indicate that polyomaviruses have the potential to be oncogenic in zebra finches.

**Abbreviations:** IHC, immunohistochemistry; NGS, next-generation sequencing; ISH, in situ hybridization; rpm, reads per million

DOI: 10.30802/AALAS-CM-23-000011

## Introduction

Lymphoid neoplasia is the most common form of hemolymphatic malignancy in avian species.<sup>5</sup> In a recent retrospective review of avian necropsy cases at a major academic institution, 22% of neoplasms were diagnosed as lymphoma.<sup>18</sup> The majority of these cases were multicentric and most prevalent in Psittaciformes, followed by Galliformes, and, finally, Passeriformes.<sup>18</sup> Lymphoma is also the most common form of lymphoid neoplasia in the psittacine and passerine species.<sup>5</sup> It usually originates in primary or secondary lymphoid tissues and disseminates to other locations in the body. Lymphoid leukemia is another form that develops in the bone marrow and then disseminates throughout the body.<sup>5</sup> This manifestation is not commonly recognized in pet bird species, likely because by the time most necropsies occur, diffuse disease is present, and determining the organ of origin is challenging.<sup>5</sup>

Viral-induced lymphoproliferative disease has been well-documented in some avian species.<sup>5,8</sup> Gallid Herpesvirus 2 (GaHV-2; Marek's disease virus) is an  $\alpha$ -herpesvirus that typically induces a T-cell lymphoma in which lymphocytes invade nerve trunks, ocular tissues, feather follicles, and internal organs.<sup>5,15</sup> Avian leukosis virus (ALV) is a retrovirus that induces a B-cell lymphoma with infiltration of lymphoblastic cells most frequently into the liver, spleen, kidneys, and bursa of Fabricius.<sup>5,15</sup> Reticuloendotheliosis virus (REV) is a retrovirus that induces either a B- or T-cell lymphoma with infiltration most commonly of the intestinal tract, liver, and spleen.<sup>5,8</sup> Lymphoid neoplasia in psittacine and passerine species is suspected to be viral-induced, but to date, none of the aforementioned viruses have been identified in these species. A male European starling (*Sturnus vulgaris*) that was diagnosed with multicentric lymphoma was found to have a *pol*-specific sequence in neoplastic tissue, suggestive of a retroviral cause, but polymerase chain reaction (PCR) assays were negative for REV and ALV.<sup>27</sup> Polyomaviruses have not typically been associated with lymphoma or tumors in avian species but instead typically produce acute inflammatory diseases with high mortality rates or chronic disease characterized by feather disorders.<sup>9,12</sup> The current report documents disseminated T-cell lymphoma in a colony of zebra finches that appears to be linked with a polyomavirus that has not been described previously in this species.

Submitted: 22 Feb 2023. Revision requested: 13 Mar 2023. Accepted: 20 Jun 2023.

<sup>1</sup>Division of Comparative Medicine, Department of Pathology, Microbiology and Immunology, Vanderbilt University Medical Center, Nashville, Tennessee, <sup>2</sup>Department of Biological Sciences, Vanderbilt University, Nashville, Tennessee, <sup>3</sup>Cornell University College of Veterinary Medicine, Ithaca, New York, <sup>4</sup>Cornell Institute of Biotechnology, Transcriptional Regulation and Expression Facility, Ithaca, New York

\*Corresponding author. Email: katherine.shuster@vumc.org

## Case Report

**Animals.** Vanderbilt University maintains a colony of approximately 150 zebra finches (*Taeniopygia guttata*) that are used to study the effects of stress on song development. The zebra finches are housed in an AAALAC-accredited animal facility and are part of an IACUC-approved research protocol. The birds are maintained on a 12:12-h light:dark cycle, with temperatures ranging from 68 to 77 °F (20 to 25 °C) and relative humidity of 20% to 80%. A fortified seed mix (Supreme Finch Diet, Kaytee, Chilton, WI) is provided ad libitum. Breeding animals also receive “egg food” consisting of crushed hard-boiled chicken eggs mixed with a dietary supplement (Exact Hand Feeding Formula, Kaytee), calcium supplement (Avian Calcium, Zoo Med Laboratories, San Luis Obispo, CA), and vitamin supplement (Avian Plus Vitamin and Mineral Supplement, Zoo Med Laboratories). Municipal water in bottles and cuttlebones are always available. Millet sprays are provided for foraging enrichment. The birds are housed in breeding pairs, small groups, or individually when on study or receiving treatment. The birds are housed in standard rectangular bird enclosures with wire bars and solid pans with a paper liner to facilitate cleaning. Nest boxes and species-appropriate nesting material (burlap fiber or coconut fiber) are provided for breeding animals.

The founders were obtained from a single source and no new birds have been introduced into the colony since the original founders in the fall of 2017. The founder colony consisted of 37 birds (18 males, 19 females) that we obtained from a lab that studied sexual dimorphism of the song system. Those studies involved sex hormone manipulation during development and in adults and local knockdown of Z-chromosome genes. Only one of the original founders currently remains in the colony.

**Case 1.** A 3-y-old female zebra finch from the founder colony presented with nonspecific clinical signs, including ruffled feathers and shivering. This bird had no known experimental history and had been socially housed before presentation, at which point she was housed individually to facilitate the provision of daily supportive care, including egg food and access to a heat lamp placed outside one side of the enclosure. This bird appeared to respond well to the supportive care during this time because she was active and exhibited normal eating, flying, and perching. After 3 wk of receiving the supportive care measures, the bird was found dead and submitted for necropsy.

**Case 2.** A 1.5-y-old female zebra finch bred in-house presented with ruffled feathers and nonweight-bearing lameness on the left leg. This bird had no known experimental history. A skin lesion with mild swelling was noted on the plantar surface of the left foot, with dried blood and debris surrounding the lesion. The foot was cleaned, and treatment with a triple antibiotic ointment was initiated based on the diagnosis of a superficial wound. The bird was bright/alert/responsive and able to fly, perch, and ambulate. The bird was started on daily supportive care, including the provision of egg food, nesting material, and padded perches. The next day, the bird was found dead and submitted for necropsy.

**Case 3.** A 4.5-y-old male zebra finch bred in-house presented with masses around the head and feather loss. As a nestling, this finch had undergone nutritional stress treatment via food restriction as part of the IACUC-approved protocol. The lab elected to euthanize this animal using IACUC-approved protocol methods for necropsy submission.

**Case 4.** A 3.5-y-old male zebra finch from the founder colony presented with a skin ulceration on the right ventral neck. The bird had no known experimental history. Topical treatment with triple antibiotic ointment was initiated, but no improvement was noted. The finch then received an oral antibiotic (trimethoprim-sulfamethoxazole) once daily (0.96 mg/day) for 10 d. No external parasites were seen, and no growth occurred on a swab sample taken from the affected area for aerobic culture and sensitivity. The skin lesion appeared smaller after completion of the oral antibiotic therapy, and the bird appeared otherwise healthy. One week later, the bird was found dead and submitted for necropsy.

## Materials and Methods

**Necropsy and histopathology.** Necropsy and immunohistochemistry were overseen by board-certified veterinary anatomic pathologists. Tissues were fixed in 10% neutral buffered formalin at the time of necropsy. A complete set of fixed tissues was trimmed and routinely processed using a standard 8-h processing cycle of graded alcohols, xylenes, and paraffin wax, embedded and sectioned at 4 to 5 microns, floated on a water bath, and mounted on adhesive glass slides. Hematoxylin and eosin staining was performed on the Gemini autostainer (Thermo Fisher Scientific, Waltham, MA).

**Immunohistochemistry.** For all immunostaining, a set of nonlesioned zebra finch control tissues containing mixed immune cell populations was used to identify positive and negative labeling as compared with the normal validated control tissues that are typically run with each antibody. All immunohistochemical (IHC) staining was performed by the Translational Pathology Shared Resource at Vanderbilt University Medical Center. One or 2 representative sections were selected from each case for both CD3 and Pax5 IHC.<sup>7</sup> Details for both antibodies and staining protocols are listed in Table 1. Before the IHC assay, select tissue sections underwent similar processing and slides underwent serial dehydration and clearing with xylene. All IHC staining was performed on a Leica BOND Rx autostainer (Leica Biosystems, Deer Park, IL), which included peroxide blocking, retrieval, and primary antibody incubation. The Bond Polymer Refine detection system (Leica Biosystems) was used for visualization. Slides were then dehydrated, cleared, and coverslipped.

**Acid-fast staining.** Acid-fast staining was performed in Vanderbilt University Medical Center’s Translational Pathology Shared Resource. Slides were deparaffinized and incubated with carbol fuchsin followed by acid alcohol. The slides were then washed and incubated with methylene blue (Artisan Acid-Fast *Bacillus* Stain Kit AR162, Agilent Technologies, Santa Clara, CA).

**Next-generation sequencing.** Total nucleic acid was extracted from formalin-fixed paraffin-embedded (FFPE) tissue

**Table 1.** IHC reagents and protocols

Epitope	Target	Manufacturer	Species	Dilution	Clonality	Incubation time	Lab-validated species
CD3	Pan-T-cell	Abcam	Rabbit	1:250	Monoclonal	60 min	Mouse
Pax5	B cell	Leica	Mouse	Not diluted; provided in ready-to-use form	Monoclonal	60 min	Mouse

(RecoverAll kit, Thermo Fisher Scientific) and frozen (MagMAX AM1840 kit, Thermo Fisher Scientific) liver tissue and submitted to the Transcriptional Regulation and Expression Facility (Cornell Institute of Biotechnology, Ithaca, NY) for RNA sequencing. After rRNA depletion with the RiboZero HMR kit (Illumina, San Diego, CA), RNA sequencing libraries were generated using the NEBNext Ultra II Directional Library Prep kit (New England Biolabs, Ipswich, MA), quality checked, and sequenced on the Illumina iSeq and NextSeq 500 platforms. Trimmed reads were initially assembled using rnaSPAdes and run against the National Center for Biotechnology Information Nucleotide database using Kraken2 to identify candidate viruses. Read metrics and consensus genomes were generated using the Chan Zuckerberg ID pipeline,<sup>14</sup> where raw sequences and assembled genomes are available for download (<https://czid.org/>) under project Zebrafinch. All data are also available at NCBI under BioProject PRJNA935364.

**RNAscope in situ hybridization.** Six blocks were selected from all zebra finch tissues that contained lymphoproliferative lesions and were used to probe for virus using RNAscope in situ hybridization (ISH). Based on the next-generation sequencing (NGS) results from the frozen liver tissue, a proprietary 20ZZ probe was designed to target the VP1 gene of the sequenced polyomavirus (within positions 2027 to 3079 of GenBank accession KY986580.1). A housekeeping probe (Tgu-PPIB) was used to ensure RNA quality in all tested tissues. All RNAscope assays were performed on a Leica BOND Rx IHC autostainer (Leica Biosystems) according to manufacturer's instructions (RNAscope 2.5 LS Assay-Red, Advanced Cell Diagnostics, Newark, CA).

## Results

**Case 1.** On gross necropsy, the bird weighed 15 g, had a body condition score (BCS) of 2/5,<sup>21</sup> and was in fair condition. Approximately a dozen petechiae were present on the skin of the ventral body and scattered pinpoint excoriations were seen along the dorsum. The crop was empty. Scant yellow flecks were noted in the thoracic wair sacs. A culture swab was collected from the thoracic air sacs and submitted for aerobic and fungal cultures, which were performed by the Athens Veterinary Diagnostic Laboratory at the University of Georgia; these cultures were negative. The right lobe of the liver was broadly and firmly adhered to the right side of the body wall and small and large intestines; this finding was interpreted initially as chronic coelomitis (Table 2).

Histopathology demonstrated a disseminated, anaplastic round cell neoplasm affecting the coelom, lungs, heart, skeletal muscle, proventriculus, ventriculus, small intestine, large intestine, liver, bursa of Fabricius, spleen, kidneys, skin, and reproductive tract (Figure 1A). In skin, the neoplastic cells demonstrated epitheliotropism (data not shown) or demonstrated angioinvasion in skeletal muscle and lung (Figure 1B). Neoplastic cells had distinct cell borders, small amounts of eosinophilic cytoplasm, large nuclei with coarsely stippled chromatin, and variably distinct nucleoli. The neoplasm showed moderate to marked anisocytosis and anisokaryosis, with 1 to 2 mitotic figures observed per 10 high-powered fields. These features, combined with the cytologic characteristics, were most consistent with high-grade lymphoma. Acid-fast staining conducted for mycobacterial screening was negative.

CD3 and Pax 5 immunostains were performed to differentiate between T- and B-cell neoplasms, respectively.<sup>7</sup> CD3 IHC revealed strong membranous staining of over 80% of the neoplastic round cells, with only a small subset (< 20%) showing moderate nuclear staining for Pax5, supporting a diagnosis of T-cell lymphoma.<sup>7</sup> RNAscope ISH for the polyomavirus showed robust signals disseminated throughout and scattered around neoplastic clusters (Figure 2A).

**Case 2.** On gross necropsy, the bird weighed 12 g, had a BCS of 2/5,<sup>21</sup> and was in fair condition. The bird had marked hepatomegaly; the liver weighed 2 g (16% of body weight). Liver samples were frozen at -80 °C for possible future diagnostics.

Histopathology demonstrated a disseminated round cell neoplasm affecting all viscera. Unique to this case, the neoplastic cells involved and invaded serosal surfaces and the lamina propria of the ventriculus. Putative intranuclear inclusions were disseminated among neoplastic cells (Figure 1C). Intranuclear inclusions were glassy and amphophilic with chromatin margination. Cellular features of the neoplastic cells were similar to those of case 1 and were occasionally mixed with small to moderate numbers of tingible body macrophages. Due to the finding of intranuclear inclusions on histopathology, a viral etiology was suspected, prompting NGS.

The data from this sample mapped with 100% sequence homology to *Serinus canaria* polyomavirus (Figure 3A) strain 34639 (GenBank accession KY986580.1),<sup>22</sup> which was originally identified in a European goldfinch, with 99% coverage of the genome at an average depth of 37.8× and with 83.7 matching reads per million quality-filtered reads (rpm; Figure 3B). Additional findings from the untargeted RNAseq with homology

**Table 2.** Clinical and gross findings

Case	Signalment	Clinical signs	Necropsy date	Gross findings
1	3-y-old female founder; no known experimental use	Ruffled feathers and shivering	7/18/18	Petechiae on the ventral body; pinpoint excoriations on the dorsum; scant yellow flecks in the thoracic air sacs
2	1.5-y-old female bred in-house; no known experimental use	Ruffled feathers and nonweight-bearing lameness on the left leg	10/24/19	Marked hepatomegaly
3	4.5-y-old male bred in-house; used for study of nutritional stress via food restriction as a nestling	Feather loss and masses around the head	7/14/22	Multifocal to coalescing bulging masses that were tan to yellow in color with variable loss of feathers and erosion/ulceration of the skin of the head; marked hepatomegaly
4	3.5-y-old male founder; no known experimental use	Skin ulceration on the right ventral neck	2/18/19	Marked circumferential feather loss on the neck with multiple small foci of thickening and excoriation; liver was mottled light to dark red throughout; testes were asymmetric

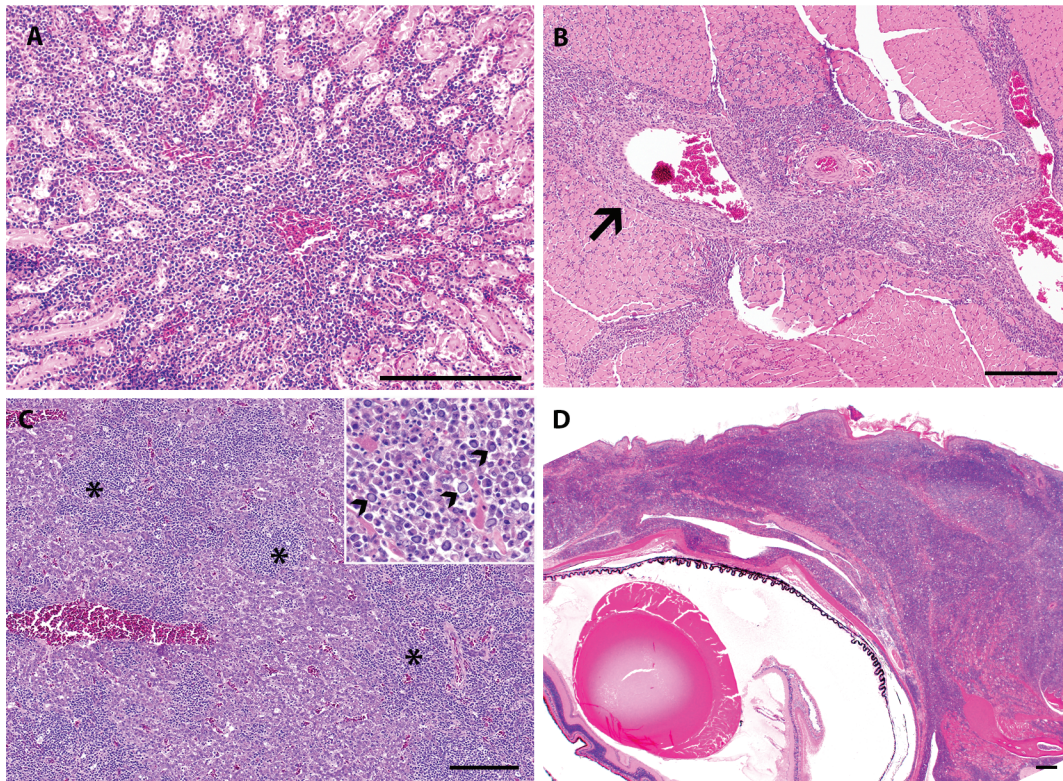


**Figure 1.** Disseminated lymphoma infiltrates various zebra finch tissues, including (A) kidney, infiltrating the renal interstitium (case 1); (B) skeletal muscle, with angioinvasion (arrow) (case 1); (C) liver, forming multiple nodules (asterisks) with intranuclear inclusion bodies (inset, arrowheads) (case 2); and (D) skin, expanding the dermis on the head and effacing the periocular glands (case 3). Hematoxylin and eosin (H and E) stain, Bar = 200  $\mu$ m.

to nucleotide sequences in NCBI included *Lonchura striata* deltavirus (114.8 rpm with 93.6% coverage of GenBank accession LC575944.1) and an unspecified mitovirus (9.6 rpm). Based on protein homology only, the black Syrian hamster retrovirus and avian sarcoma virus were also identified at very low levels.

In areas with solid tumor formation, approximately 70% of the neoplastic cells immunolabeled with CD3 mixed with small aggregates of cells labeled for Pax 5. Given the staining pattern and combined with histomorphology, the diagnosis was most consistent with T-cell lymphoma.<sup>7</sup> Similar to case 1, RNAscope polyomavirus ISH revealed disseminated signals concentrated in regions with neoplastic cell clusters (Figure 2B).

**Case 3.** On gross necropsy, the head had multifocal to coalescing bulging masses that were tan to yellow in color, with variable loss of feathers and erosion/ulceration of the skin of the head. The bird also had marked hepatomegaly.

On histopathology, a round cell neoplasm was seen to be affecting the subcutaneous tissues of the head, the dermis and underlying skeletal muscle, periocular glands (Figure 1D), salivary glands, proximal trachea, and skull. A large proportion of the neoplastic cells contained intranuclear inclusion bodies. Moderate extramedullary hematopoiesis was noted throughout the liver, primarily centered around portal zones, and was likely a reaction to the presence of a hematopoietic neoplasm.

IHC staining results were similar to those of case 2, in which up to 70% to 80% of the neoplastic cells were immunolabeled for CD3 and 10% to 15% tested positive for Pax 5; the latter cells often appeared in small clusters. RNAscope ISH signals for polyomavirus were abundant in neoplastic nodules and were also present in the sinusoids of the liver (Figure 2C).

**Case 4.** On gross necropsy, the bird weighed 14 g, had a BCS of 3/5,<sup>21</sup> and was in fair condition. Marked circumferential feather loss was present around the neck, with multiple small foci of skin thickening and excoriation. The crop was empty, and no grit was present in the ventriculus. The liver was mottled light to dark red throughout. The testes were asymmetric, with the left measuring 4 mm in diameter and the right measuring 2 mm in diameter.

On histopathology, neoplastic round cells occurred in variably sized aggregates scattered in multiple organs, including the kidneys, liver, heart (pericardium and epicardium), lungs, and peritoneum. The neoplasm had also infiltrated and markedly expanded the dermis around the head and neck, accompanied by multiple dermal ulcerations with large colonies of cocci bacteria, mixed inflammation, and multifocal necrosis. Large numbers of cells within neoplastic clusters contained intranuclear inclusion bodies, most prominently in the lungs and skin. Cellular features were similar to the neoplasms described above, with marked pleomorphism noted in the dermal population.

In the skin, up to 70% of the neoplastic cells immunolabeled with CD3 intermixed with scattered cells that stained positive for Pax5. RNAscope ISH signals for polyomavirus were abundant and robust, often in areas where neoplasms were present (Figure 2D).

Scrolls from FFPE tissue were submitted for NGS. Data from this sample mapped well (97.2% sequence homology) to *Serinus canaria* polyomavirus strain 37273, which was originally isolated from a canary (GenBank accession KY986581.1),<sup>22</sup> with 77.4% coverage of the genome at an average depth of 7.7 $\times$  and 75.2 rpm (Figure 4).

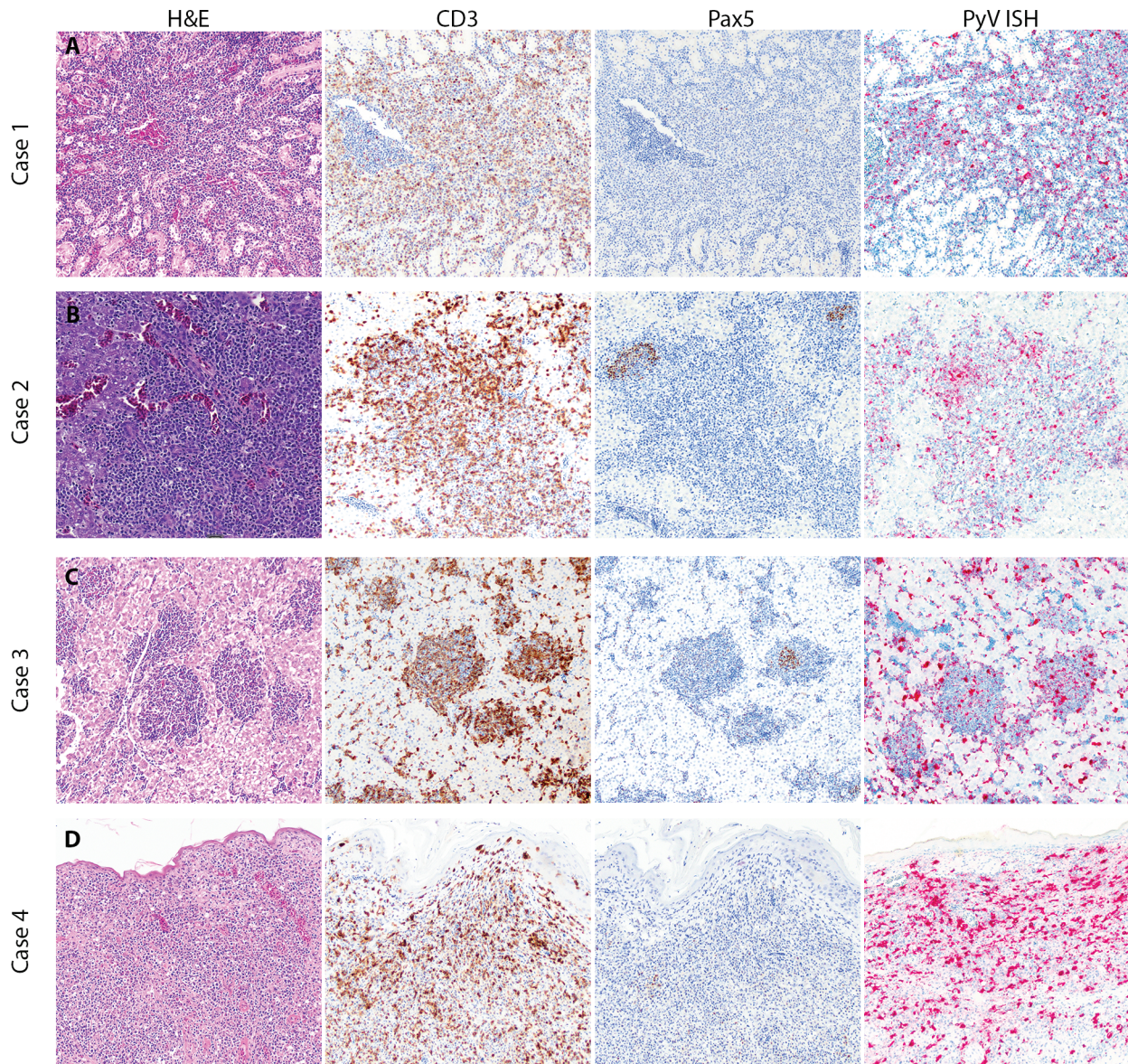


**Figure 2.** Results for immunohistochemistry (CD3 and Pax 5) and RNAscope in situ hybridization using a polyomavirus-specific probe. Panels show corresponding H and E sections from (A) case 1, (B) case 2, (C) case 3, and (D) case 4. Up to 70% to 80% of neoplastic cells were immunopositive for CD3 (brown), supporting a diagnosis of T-cell lymphoma in all 4 cases. Robust hybridization signals (red) for polyomavirus can be seen disseminated throughout the neoplastic tissues in all cases.

**Colony monitoring.** Round cell neoplasia consistent with lymphoma with associated intranuclear inclusions continues to be diagnosed sporadically (approximately 12% prevalence, 18 total cases) in our zebra finch colony.

## Discussion

This report details the findings of disseminated T-cell lymphoma in our colony of zebra finches; the lymphoma appears to be linked to *Serinus canaria* polyomavirus.<sup>22</sup> To our knowledge, this is the first literature report on disseminated T-cell lymphoma in the zebra finch. Several other tumor types have been documented in this species, including intestinal leiomyosarcoma,<sup>2</sup> malignant melanoma,<sup>11</sup> myelolipoma,<sup>25</sup> and subcutaneous hemangiosarcoma.<sup>25</sup> T-cell lymphoma has been confirmed in several other avian species, including a great horned owl (*Bubo virginianus*) that presented with stridor and weight loss,<sup>15</sup> a Catalina macaw (*Ara ararauna x Ara macao*) that

presented with bilateral uveitis and hyphema,<sup>10</sup> a roller pigeon (*Columba livia*) that presented with acute left limb lameness,<sup>28</sup> a Humboldt penguin (*Spheniscus humboldti*) that presented with dysphagia,<sup>23</sup> and a pink-backed pelican (*Pelecanus rufescens*) that was found dead with no prior clinical signs.<sup>23</sup> In the case of the Catalina macaw, Humboldt penguin, and pink-backed pelican, test results were negative for the 3 most common avian lymphoproliferative viruses.

Polyomaviruses are small, nonenveloped, double-stranded DNA viruses in the family *Polyomaviridae*. They are found in a wide variety of vertebrates and are comprised of circular, double-stranded DNA approximately 5000bp in length that encodes 5 main proteins: 2 regulatory proteins known as large and small T antigens and 3 structural proteins (VP1, VP2, and VP3) that make up the icosahedral viral capsid.<sup>16,20</sup> Avian polyomaviruses do not encode a middle T antigen but generally encode VP4 or a homologous protein and are separate phylogenetically from mammalian polyomaviruses.<sup>12</sup> They

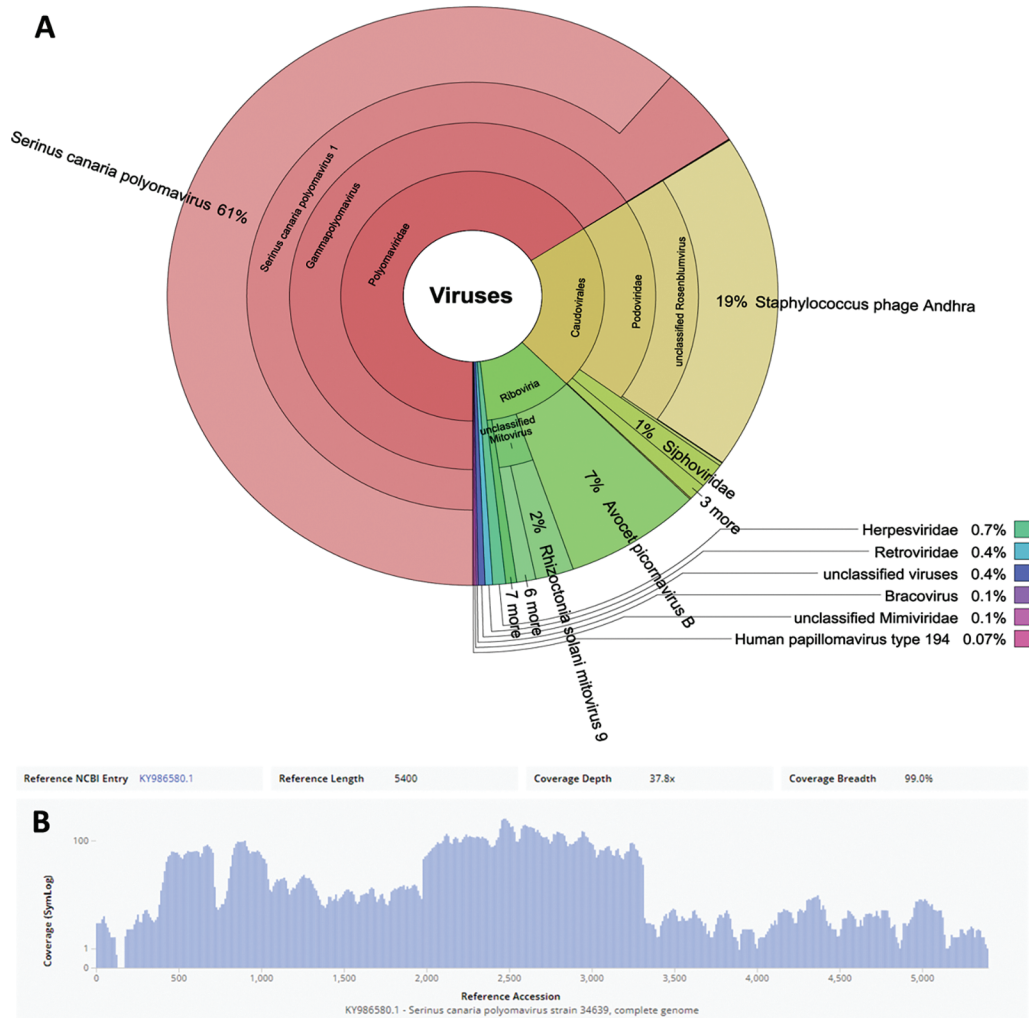


**Figure 3.** Krona plot (A) of viral reads from the next-generation sequencing (NGS) testing on the frozen liver tissue from case 2, demonstrating that this sample mapped well (100% sequence homology) to *Serinus canaria* polyomavirus, specifically strain 34639 (GenBank accession KY986580.1) from a European goldfinch, with 99% coverage of the genome at an average depth of 37.8× and 83.7 matching reads per million quality-filtered reads (B).

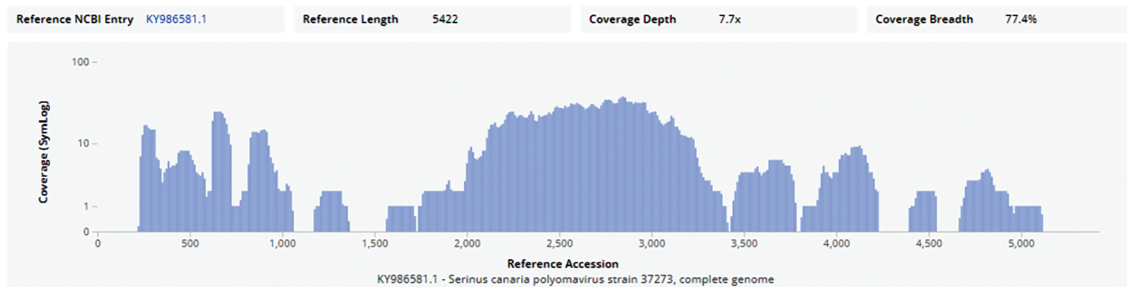


**Figure 4.** NGS data from case 4 mapped well (97.2% sequence homology) to *Serinus canaria* polyomavirus strain 37273 from a canary (GenBank accession KY986581.1), with 77.4% coverage of the genome at an average depth of 7.7× and 75.2 rpm.

are classified under the genus Gammapolyomavirus, whereas species in the genera Alphapolyomavirus, Betapolyomavirus, and Deltapolyomavirus only infect mammals.<sup>1</sup>

Avian polyomaviruses are not typically associated with lymphoma or tumors.<sup>9,12,13</sup> Clinical signs seen in infected finches typically include sudden death, emaciation, lethargy, diarrhea, dyspnea, and feather disorders (e.g., loss of feathers on the head).<sup>22</sup> One published report describes an adult female zebra finch that presented with unilateral periorbital swelling and

nodules on the neck, thorax, and wings.<sup>19</sup> Gross necropsy revealed that the crop, skeletal and cardiac muscles, intestine, and mesentery were also affected. On histopathology, the nodules were comprised of dense sheets of poorly differentiated neoplastic cells with intranuclear inclusions. PCR was performed on frozen tissue samples. Two novel polyomaviruses were found; they were most similar to canary and crow strains.<sup>19</sup> Mammalian polyomaviruses have been implicated in inducing neoplasia in the host,<sup>17</sup> with hamsters providing a well-known example

of lymphoma induction.<sup>3,26</sup> The large T antigen in most avian polyomaviruses contains the sequence necessary for binding to the tumor suppressor protein pRB.<sup>13,16</sup> In vitro studies have shown that avian polyomaviruses can transform mammalian cells but they have not been shown to induce tumors in the natural host or other animals to date.<sup>13,16</sup>

Our NGS findings revealed other viruses at a low level in the analyzed tissue. The presence of polyomavirus at high levels in these tissues, the detection of intranuclear inclusions and robust ISH signals of viral nucleic acids in neoplastic tissues, together with the fact that virus is known to induce tumors in other species<sup>3,17,26</sup> strongly suggest that the polyomavirus caused the lesions noted. A limitation of the current study is that only one of the 2 samples submitted for NGS came from frozen tissue. Total nucleic acid extraction from FFPE samples can be difficult and may have led to incomplete NGS data in that particular case. Further characterization of the virus in our colony is a possible topic for future study.

We now know that disseminated T-cell lymphoma is present in some birds in our zebra finch colony and appears to be associated with enzootic infection with a polyomavirus. We suspect that clinical disease may occur if infected birds become immunosuppressed (e.g., advanced age, concurrent illness), leading to reactivation of the virus, as occurs during infection with mammalian polyomaviruses.<sup>16</sup> Due to the unavailability of clinical diagnostic tests for passerine species, we cannot screen our colony to learn the true prevalence of this virus. Continued work in diagnostic testing and research into the avian virome<sup>4,6,24</sup> would help to further elucidate the potential role of this virus in tumor induction in avian species.

## Acknowledgments

The Translational Pathology Shared Resource is supported by NCI/NIH Cancer Center Support Grant 5P30 CA68485-19 and IHC studies were completed using the Leica Bond Rx autostainer supported by the Shared Instrumentation Grant S10 OD023475. We thank the Molecular Diagnostics Laboratory at the Animal Health Diagnostic Center at Cornell University College of Veterinary Medicine and the Cornell Transcriptional Regulation and Expression Facility for performing the NGS for samples from these cases. NC and KTS are supported by the National Science Foundation (BCS-1918824) and this grant also funds the maintenance of the studied zebra finch colony.

## References

1. Calvignac-Spencer S, Feltkamp MCW, Daugherty MD, Moens U, Ramqvist T, Johne R, Ehlers B, Polyomaviridae Study Group of the International Committee on Taxonomy of Viruses. 2016. A taxonomy update for the family Polyomaviridae. *Arch Virol* **161**:1739–1750. <https://doi.org/10.1007/s00705-016-2794-y>.
2. Cardoso JFR, Levy MGB. 2014. Pathological and Immunohistochemical Diagnosis of an Intestinal Leiomyosarcoma in a Zebra Finch. *Braz J Vet Pathol* **7**:89–92.
3. Cassano A, Rasmussen S, Wolf FR. 2012. Viral Diseases in Hamsters, p 822-825. In: Suckow MA, Stevens KA, Wilson RP, editors. *The Laboratory Rabbit, Guinea Pig, Hamster, and Other Rodents*. Waltham, MA: Academic Press.
4. Chang W-S, Eden J-S, Hall J, Shi M, Rose K, Holmes EC. 2020. Metatranscriptomic Analysis of Virus Diversity in Urban Wild Birds with Paretic Disease. *J Virol* **94**:e00606–e00620. <https://doi.org/10.1128/JVI.00606-20>.
5. Coleman CW. 1995. Lymphoid Neoplasia in Pet Birds: A Review. *J Avian Med Surg* **9**:3–7.
6. François S, Pybus OG. 2020. Towards an understanding of the avian virome. *J Gen Virol* **101**:785–790. <https://doi.org/10.1099/jgv.0.001447>.
7. Gibson DJ, Nemeth NM, Beaufrère H, Varga C, Garner MM, Susta L. 2021. Lymphoma in Psittacine Birds: A Histological and

Immunohistochemical Assessment. *Vet Pathol* **58**:663–673. <https://doi.org/10.1177/03009858211002180>.

8. Haesendonck R, Garmyn A, Dorrestein GM, Hellebuyck T, Antonissen G, Pasmans F, Ducatelle R, Martel A. 2015. Marek's disease virus associated ocular lymphoma in Roulroul partridges (*Rollulus rouloul*). *Avian Pathol* **44**:347–351. <https://doi.org/10.1080/03079457.2015.1056088>.
9. Halami MY, Dorrestein GM, Couteel P, Heckel G, Müller H, Johne R. 2010. Whole-genome characterization of a novel polyomavirus detected in fatally diseased canary birds. *J Gen Virol* **91**:3016–3022. <https://doi.org/10.1099/vir.0.023549-0>.
10. Hausmann JC, Mans C, Gosling A, Miller JL, Chamberlin T, Dunn JR, Miller PE, Sladky KK. 2016. Bilateral Uveitis and HypHEMA in a Catalina Macaw (*Ara ararauna* × *Ara macao*) With Multicentric Lymphoma. *J Avian Med Surg* **30**:172–178. <https://doi.org/10.1647/2015-105>.
11. Irizarry-Rovira AR, Lennox AM, Ramos-Vara JA. 2007. Malignant melanoma in a zebra finch (*Taeniopygia guttata*): cytologic, histologic, and ultrastructural characteristics. *Vet Clin Pathol* **36**:297–302. <https://doi.org/10.1111/j.1939-165X.2007.tb00229.x>.
12. Johne R, Müller H. 2007. Polyomaviruses of birds: etiologic agents of inflammatory diseases in a tumor virus family. *J Virol* **81**:11554–11559. <https://doi.org/10.1128/JVI.01178-07>.
13. Johne R, Wittig W, Fernández-de-Luco D, Höfle U, Müller H. 2006. Characterization of two novel polyomaviruses of birds by using multiply primed rolling-circle amplification of their genomes. *J Virol* **80**:3523–3531. <https://doi.org/10.1128/JVI.80.7.3523-3531.2006>.
14. Kalantar KL, Carvalho T, Bourcy CFA de, Dimitrov B, Dingle G, Egger R, Han J, Holmes OB, Juan Y-F, King R, Kislyuk A, Lin MF, Marian M, Morse T, Reynoso LV, Rissato Cruz D, Sheu J, Tang J, Wang J, Zhang MA, Zhong E, Ah Yong V, Lay S, Chea S, Bohl JA, Manning JE, Tato CM, DeRisi JL. 2020. IDseq-An open source cloud-based pipeline and analysis service for metagenomic pathogen detection and monitoring. *Gigascience* **9**:giaa111. <https://doi.org/10.1093/gigascience/giaa111>.
15. Malka S, Crabbs T, Mitchell EB, Zehnder A, Kent MS, Lowenstine LJ, Hawkins MG. 2008. Disseminated lymphoma of presumptive T-cell origin in a great horned owl (*Bubo virginianus*). *J Avian Med Surg* **22**:226–233. <https://doi.org/10.1647/2007-048.1>.
16. Moens U, Krumbholz A, Ehlers B, Zell R, Johne R, Calvignac-Spencer S, Lauber C. 2017. Biology, evolution, and medical importance of polyomaviruses: An update. *Infect Genet Evol* **54**:18–38. <https://doi.org/10.1016/j.meegid.2017.06.011>.
17. Morgan GJ. 2014. Ludwik Gross, Sarah Stewart, and the 1950s discoveries of Gross murine leukemia virus and polyoma virus. *Stud Hist Philos Biol Biomed Sci* **48 Pt B**:200–209.
18. Nemeth NM, Gonzalez-Astudillo V, Oesterle PT, Howerth EW. 2016. A 5-Year Retrospective Review of Avian Diseases Diagnosed at the Department of Pathology, University of Georgia. *J Comp Pathol* **155**:105–120. <https://doi.org/10.1016/j.jcpa.2016.05.006>.
19. Patterson MM, Fee MS. 2015. Zebra Finches in Biomedical Research, p 1123. In: Fox JG, Anderson LC, Otto G, Pritchett-Corning KR, Whary MT, editors. *Laboratory Animal Medicine*. Waltham (MA): Academic Press.
20. Pérez-Losada M, Christensen RG, McClellan DA, Adams BJ, Viscidi RP, Demma JC, Crandall KA. 2006. Comparing phylogenetic codivergence between polyomaviruses and their hosts. *J Virol* **80**:5663–5669. <https://doi.org/10.1128/JVI.00056-06>.
21. Pollock C. [Internet]. 2012. Body Condition Scoring in Birds. [Cited 17 February 2023]. Available at: <https://lafieber.com/vet/body-condition-scoring/>.
22. Rinder M, Schmitz A, Peschel A, Moser K, Korbel R. 2018. Identification and genetic characterization of polyomaviruses in estrildid and fringillid finches. *Arch Virol* **163**:895–909. <https://doi.org/10.1007/s00705-017-3688-3>.
23. Schmidt V, Philipp H-C, Thielebein J, Troll S, Hebel C, Aupperle H. 2012. Malignant lymphoma of T-cell origin in a Humboldt penguin (*Spheniscus humboldti*) and a pink-backed pelican (*Pelecanus rufescens*). *J Avian Med Surg* **26**:101–106. <https://doi.org/10.1647/2011-017.1>.

24. **Shan T, Yang S, Wang H, Wang H, Zhang J, Gong G, Xiao Y, Yang J, Wang X, Lu J, Zhao M, Yang Z, Lu X, Dai Z, He Y, Chen X, Zhou R, Yao Y, Kong N, Zeng J, Ullah K, Wang X, Shen Q, Deng X, Zhang J, Delwart E, Tong G, Zhang W.** 2022. Virome in the cloaca of wild and breeding birds revealed a diversity of significant viruses. *Microbiome* **10**:60. <https://doi.org/10.1186/s40168-022-01246-7>.
25. **Shientag LJ, Garlick DS, Galati E.** 2016. Amyloidosis in a Captive Zebra Finch (*Taeniopygia guttata*) Research Colony. *Comp Med* **66**:225–234.
26. **Simmons JH, Riley LK, Franklin CL, Besch-Williford CL.** 2001. Hamster Polyomavirus Infection in a Pet Syrian Hamster (*Mesocricetus auratus*). *Vet Pathol* **38**:441–446. <https://doi.org/10.1354/vp.38-4-441>.
27. **Wade LL, Polack EW, O'Connell PH, Starrak GS, Abou-Madi N, Schat KA.** 1999. Multicentric Lymphoma in a European Starling (*Sturnus vulgaris*). *J Avian Med Surg* **13**:108–115.
28. **Williams SM, Williams RJ, Gogal RM Jr.** 2017. Acute Lameness in a Roller Pigeon (*Columba livia*) with Multicentric Lymphosarcoma. *Avian Dis* **61**:267–270. <https://doi.org/10.1637/11577-010317-Case.1>.